

We wish to thank the referees, B.-M. Sinnhuber and C. Sioris, for their very helpful comments, corrections and suggested improvements in the manuscript. We will, of course, incorporate corrections and comments into the final version of the manuscript. Our reply to specific points follow.

Reply to general comments of referee 1 (B.-M. Sinnhuber):

- Paragraph 1: The Br_y profile (plotted in our Figures 8 and 13) is scaled from the correlation with CFC-11 in Wamsley et al., (1998) which includes CH_3Br and halons as identified in Wamsley et al.(1998 ,Table 4) and as plotted in McLinden et al. (2010, Figure 17). We will clarify this point in the final text. Varying trends in the various bromine source gases with differing photochemical lifetimes could potentially affect the Br_y vertical profile and inferred VLSL abundance. However, given that the predominant source is CH_3Br it would seem that a large change in the distribution in the other minor sources gases would be needed to change the Br_y beyond the uncertainty range in Wamsley et al.(1998). The leveling and slow decline in stratospheric bromine shown in WMO(2010) might also suggest a slow change in the shape of the Br_y profile.
- Paragraph 2: The CFC-11 extra-tropics correlation with N_2O (Wamsley et al., 1998, Eq. 16) is used to show Br_y against N_2O . The N_2O profile is from SLS measurement of N_2O emission at 627.8 GHz.
- Paragraph 3: The “SLS 2007” estimate is from an earlier SLS balloon flight. We agree that this entry in Figure 14 is not sufficiently explained and will be replaced with text.
- Paragraph 4: The amplitude of the spectral residuals provides a measure of the overall quality of the retrieval. Baseline artifacts, RF and EMI interferences are (typically) the largest contributor to profile error. Δx from Eq. 5 yields the projection of the magnitude of spectral residuals into vmr. We will add text to clarify this point and a figure showing the error budget similar to that included below.

Reply to specific comments, otherwise the referee’s corrections will be adopted in the final version

- P28896L11 We will modify this text to provide more general description of the channel shape. The polyphase FFT approach provides greatly improved adjacent channel rejection as compared with $\sin(x)/x$ response of the standard FFT algorithm.
- We agree that the content of Section 2 could be merged with the Introduction and Section 3.
- P28898L25 The typesetting error in Eq.5 will be corrected. The right hand term should contain Δy not Δx

Reply to general comments of referee 2 (C. Sioris):

- Paragraph 2: The comment is that the reported profile may possibly be influenced by the a priori profile and co-variance. We show that that is not the case by evaluating, as example, the radiometric noise using Equation 6 (P28899) for the spectrum centered at 30 km tangent height. In this case, the average integration time is 1100 s, the effective signal bandwidth is 40 MHz corresponding to the mid-strat pressure-broadened BrO linewidth and system noise (receiver plus atmosphere) is 300 K. This result is approximately 0.0014 K, or 3 mK post-calibration. This yields a signal to noise estimate of 70 which significantly exceeds the estimated BrO profile error of 12%. The major contributor to profile uncertainty is therefore not radiometric noise but from systematic error as noted on P28899L20 and quantified by analysis of the spectral residuals. The stabilized actively-pointed balloon platform provides the advantage of long integration time (several hours) while viewing a (nearly) invariant scene. Composition retrievals on the low-noise averaged spectra are essentially independent of the a priori profile and covariance even for weak emission sources like BrO..
- Paragraph 3: The a priori profile can easily be added to Fig. 6 or a figure (as included below) showing the error budget (radiometric noise, calibration, residual and total) compared with the a priori and final profile. Figure 1 here shows that, over the full altitude range reported, the co-variance of the a priori is much larger than measurement co-variance and therefore retrieval result is not constrained to the a priori.

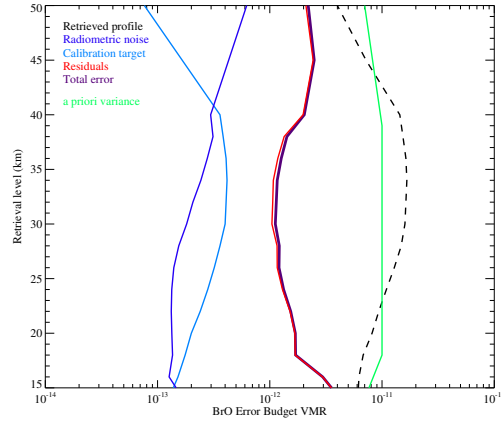


Figure 1: Plot showing the BrO profile error budget. Radiometric noise is calculated using Eq. 6 with the total integration time and signal bandwidth at each retrieval level. Calibration target error is the overall scaling uncertainty from knowledge of the calibration target radiometric temperature. Residual error is from the post-retrieval radiance residuals mapped into BrO vmr.

- Paragraph 4: At altitudes above the balloon, viewing geometry transitions from 'limb' to a shorter upward slant path. This geometry is similar to that in ground-based radiometry (however without signal attenuation due to the troposphere). Although the integration path length is reduced, the retrievals have good sensitivity except that vertical resolution above the balloon (typically 5 to 7 km) is obtained solely from linewidth. We also note, for optically thin paths, that each limb integration path includes radiance contributions from gases above the balloon as the path exits the atmosphere.
- Paragraph 5: We believe that the referee concerns of bias due to ozone variation are addressed by this clarification. Ozone emission (including the $OO^{17}O$ isotopologue and hot band) was continuously measured, simultaneously with BrO spectral emission, from a set of much stronger features near 4.5 GHz intermediate frequency (see Fig. 3). The small day-night spectral difference (approximately 0.7 K) in the region of strong O_3 emission implies a small ozone bias (approximately 10 mK) originating from the much weaker ozone features near BrO. Although the BrO region is optically thin and radiance additive, the forward radiance model corrected minor atmospheric attenuation of the BrO signal. In essence, ozone spectral features are removed by calibration (using day-night differences) and this procedure is not dependent on either a retrieved or assumed O_3 profile. In this approach, potential biases introduced by changes in either composition or temperature between day and night would appear in the residual spectra and are included in the error budget.

We state that the SLS instrument uses a double sideband receiver (P28895, L20). The 'additional' spectral features are those from the mixer lower sideband. The instrumental double sideband response is also indicated by the triple abscissa scales in Figures 03-05 which show the upper sideband, lower sideband and intermediate frequencies. SLS differs from JEM/SMILES where a sideband filter (P28894, L18) blocked signals from the lower sideband. We will also clarify in the final paper that the gondola azimuth pointing is controlled.

Regarding comments on Section 5: Equation 5 contains a typesetting error that will be corrected (right-hand side should read Δy) and we will include the clarification that in the retrieval analysis the measurement vector, Δy , is consists of individual channels of daytime-averaged spectra minus nighttime-averaged spectra for each tangent height bin.

Reply to specific comments, otherwise the referee's corrections will be adopted in the final version

- P28895L4 We will clarify that the although the receiver band is 4-8 GHz the spectrometer bandwidth is 3 GHz
- P28896L11 We will add text to explain the advantages afforded by the channel shape provided by the polyphase spectrometer over a standard FFT

- Eq. 3 this term correctly denotes that the calibrated radiance is defined as the limb path radiance minus sky path
- The measurement noise depends only on the total integration time. We will add text to indicate the limb scan time (660 s) and the individual channel noise in each limb scan spectrum. Channels were co-added reducing the spectrometer resolution to 750 kHz due to a limitation in the spectrometer on-board data storage hardware.
- Section 7.1 The gondola platform stability is measured using an on-board attitude (solid-state gyro) package to accurately align successive limb scans.
- P28901L5 The full range of atmospheric brightness observed is 280 K however a limited range of tangent heights are included in Fig.3 The text will be corrected to clarify this point.
- P28906L11 The intent is to compare these results to published OSIRIS data [McLinden et al., 2010] and MLS which cover +40 -40.
- Figure 6. the meaning of the open circles (diurnal correction) as in Figures 10 and 11 will be stated.